Molecular Crystals and Liquid Crystals

ISSN: 1542-1406 (Print) 1563-5287 (Online) Journal homepage: http://www.tandfonline.com/loi/gmcl20

4-Carboxybiphenyl and thiophene substituted porphyrin derivatives for dye-sensitized solar cell

Sadik Cogal, Sule Erten-Ela, Kasim Ocakoglu & Aysegul Uygun Oksuz

To cite this article: Sadik Cogal, Sule Erten-Ela, Kasim Ocakoglu & Aysegul Uygun Oksuz (2016) 4-Carboxybiphenyl and thiophene substituted porphyrin derivatives for dye-sensitized solar cell, Molecular Crystals and Liquid Crystals, 637:1, 87-95, DOI: 10.1080/15421406.2016.1184383

To link to this article: http://dx.doi.org/10.1080/15421406.2016.1184383

Published online: 10 Nov 2016.

MOLECULAR CRYSTALS AND LIQUID CRYSTALS
2016, VOL. 637, 87–95
http://dx.doi.org/10.1080/15421406.2016.1184383

Taylor & Francis
Taylor & Francis Group

4-Carboxybiphenyl and thiophene substituted porphyrin derivatives for dye-sensitized solar cell

Sadik Cogal[a], Sule Erten-Ela[b], Kasim Ocakoglu[c,d], and Aysegul Uygun Oksuz[e]

[a]Department of Polymer Engineering, Faculty of Engineering and Architecture, Mehmet Akif Ersoy University, Burdur, Turkey; [b]Solar Energy Institute, Ege University, Bornova, İzmir, Turkey; [c]Advanced Technology Research & Application Center, Mersin University, Yenisehir, Mersin, Turkey; [d]Department of Energy Systems Engineering, Tarsus Faculty of Technology, Mersin University, Mersin, Turkey; [e]Department of Chemistry, Faculty of Arts and Science, Suleyman Demirel University, Isparta, Turkey

ABSTRACT

Porphyrin sensitizer (Por) containing 4-carboxybiphenyl and 2-thienyl and its metallated Zn(II) derivative (ZnPor) were synthesized and investigated. The porphyrin dyes were characterized by MALDI-MS, ^{1}H NMR, UV–vis, fluorescence and cyclic voltammetry methods. It was found that using of biphenyl bridge between anchoring group and porphyrin core enhanced the conjugation length of the porphyrin macrocycle. The new porphyrin dyes were used as sensitizers in dye-sensitized solar cells (DSSCs). ZnPor-based dye sensitized solar cells yielded a short circuit photocurrent density of 3.98 mA cm^{-2}, an open circuit voltage of 500 mV, and a fill factor of 0.67, corresponding to an overall conversion efficiency (η) of 1.33%.

KEYWORDS

Porphyrin; 4-carboxybiphenyl; dye-sensitized solar cell; thiophene

GRAPHICAL ABSTRACT

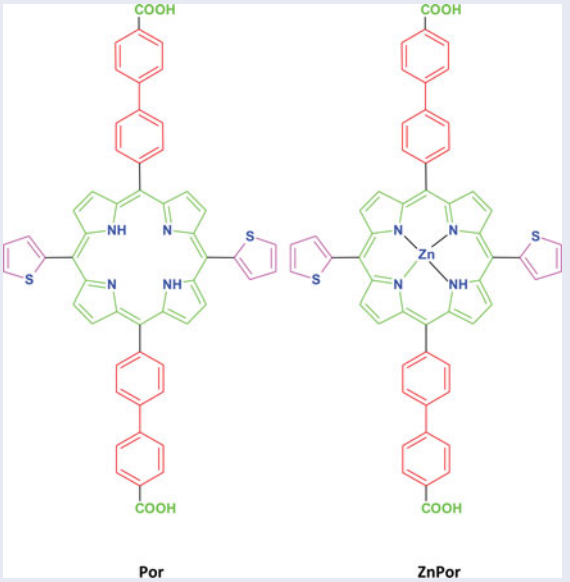

CONTACT Sadik Cogal sadik_cogal@yahoo.com Department of Polymer Engineering, Mehmet Akif Ersoy University, Faculty of Engineering and Architecture, 15030 Burdur, Turkey; Sule Erten-Ela suleerten@yahoo.com, sule.erten@ege.edu.tr Solar Energy Institute, Ege University, Bornova, 35100 Izmir, Turkey.

Color versions of one or more of the figures in the article can be found online at www.tandfonline.com/gmcl.

Introduction

Dye-sensitized solar cells (DSSCs) are emerging as one of the most promising low-cost alternative technologies to conventional inorganic photovoltaic devices [1]. Significant research efforts have been devoted to the development of new and efficient sensitizers suitable for practical use. In TiO_2-based DSSCs, ruthenium–polypyridyl complexes have been known as the most efficient sensitizers and solar cell efficiency of up to 11.4% has been achieved under simulated sunlight (AM 1.5) [2, 3]. However, the main drawback of ruthenium complexes is the lack of absorption in the red region of the visible light and the high cost. Among various organic sensitizers have been used in DSSCs, porphyrins have been extensively studied and used in DSSC due to their light-harvesting potential and suitable physicochemical properties [4]. These dyes exhibited an intense absorption around 420 nm (called Soret band) and moderate *Q* absorption bands between 550–600 nm, as well as their many reaction sites, i.e., four meso positions and eight β positions which led to obtain variety of porphyrin derivatives [5, 6]. Therefore, porphyrins are excellent alternative materials for DSSC applications and considerable research efforts have been made on the synthesis of various porphyrins and metalloporphyrins. Recently, the porphyrin dyes YD2-o-C8 and SM315 showed the highest power conversion efficiencies of 12.3% and 13%, respectively, which broke the ruthenium based DSSCs record [7, 8].

The electronic structure of porphyrin dyes, anchoring groups of dyes, the bridging distance between dye and TiO_2 particles and type of central metal are the key factors which affect the overall solar energy conversion [9–11]. To enhance the performance of porphyrin in DSSCs, the properties of porphyrin macrocycle can be tuned by introducing various substituents on the periphery of the ring, and by changing the metal center [12]. The covalent attachment of the thiophene moiety to the porphyrin macrocycle is an effective way to enhance the photophysical and electrochemical properties [13]. Ambre et al. studied the effects of number and position of *p*-carboxyphenyl and thienyl groups on zinc porphyrins based DSSCs and it was found that these changes significantly affected the performance of the device [14].

In order to move the *Q*-band absorption of porphyrin to longer wavelength, the π-electron conjugation system can be extended by using various substituents. In this study, we have designed new porphyrin dyes containing 4-carboxybiphenyl and 2-thienyl substituent and investigated their performance in DSSC. 4-Carboxybiphenyl group was selected as an anchoring moiety to the TiO_2 surface. Porphyrins were characterized using ^{1}H NMR, MALDI-MS, UV–vis, PL and CV analysis. The synthesized porphyrin dyes were applied in DSSC. ZnPor based dye sensitized solar cells gave a short circuit photocurrent density of 3.98 mA cm^{-2}, an open circuit voltage of 500 mV, and a fill factor of 0.67, corresponding to an overall conversion efficiency (η) of 1.33%.

Experimental

Materials

All materials were obtained from commercial sources and used without further purification. Pyrrole, 4-bromobenzaldehyde, 2-thienylcarboxyaldehyde, 4-methoxycarbonylphenylboronic acid, trifluoroacetic acid (TFA), tetrakis(triphenylphosphine)palladium(0) [$Pd(PPh_3)_4$], 1,2-dimethoxyethane (DME), zinc (II) acetate [$Zn(OAc)_2$], sodium carbonate (Na_2CO_3), dichloromethane, and hexane were purchased from Sigma–Aldrich. Silica

Gel 60 (0.04–0.063) was purchased from Merck. 5-(4-Bromophenyl)dipyrromethane was synthesized using a procedure by Lindsey and coworkers [15].

Synthesis of 5,15-Bis(4′-bromophenyl)-10,20-bis(2-thienyl)porphyrin (1)

5-(4-Bromophenyl)dipyrromethane (723 mg, 2.4 mmol) and 2-thienylcarboxyaldehyde (300 mg, 3.2 mmol) were dissolved in 80 mL of propionic acid. The obtained reaction mixture was heated at 110 °C under argon atmosphere for 2 hr and then the reaction mixture was allowed to cool to room temperature. The reaction mixture was neutralized with dilute NaOH and filtered. The obtained solid was dissolved in DCM and washed twice with water. DCM was evaporated under vacuum and the residue was purified by column chromatography on silica gel by using hexane:DCM (3:1) as an eluent. Compound **1** was obtained as a purple solid (200 mg, 21%). ^{1}H NMR ($CDCl_3$, 400 MHz): δ (ppm) = −2.76 (s, 2 H), 7.49–7.51 (dd, 4 H, J = 5.2 Hz), 7.85–7.92 (m, 6 H), 8.05–8.07 (d, 4 H, J = 8.0 Hz), 8.80–8.83 (m, 6 H), 9.05–9.07 (dd, 4 H, J = 8.2 Hz). MALDI TOF MS: calcd. for $C_{40}H_{24}Br_2N_4S_2$ ($[M+H]^+$) 784.580; found 785.096.

Synthesis of 5,15-Bis(4′-methoxycarbonyl-1,1′-biphenyl)-10,20-bis(2-thienyl) porphyrin (2)

Synthesis of 5,15-Bis(4′-bromophenyl)-10,20-bis(2-thienyl)porphyrin (**1**) (157 mg, 0.2 mmol), 4-methoxycarbonylphenylboronic acid (100 mg, 0.56 mmol) and $Pd(PPh_3)_4$ (23.12 mg, 0.02 mmol) were dissolved in 8 mL of DME, and stirred under argon atmosphere for 10 min. Then, 2 mL of aqueous Na_2CO_3 (21.2 mg, 0.2 mmol) was added slowly in a few portions, and the mixture was heated at 80°C for 24 hr. The reaction mixture was then allowed to cool to room temperature and the solvent was removed under vacuum. The residue was dissolved in DCM and washed twice with distilled water. DCM was evaporated under vacuum and the residue was purified by column chromatography on silica gel by using DCM:hexane (2:1) as an eluent. Compound **2** was obtained as a purple solid (35 mg, 19.5%). ^{1}H NMR ($CDCl_3$, 400 MHz): δ (ppm) = −2.66 (s, 2 H), 3.95–4.02 (m, 6 H), 7.50–7.52 (dd, 2 H, J = 5.4 Hz), 7.68–7.70 (d, 2 H, J = 8.4 Hz), 7.85–7.87 (dd, 4 H, J = 5.2 Hz), 7.93–7.94 (t, 4 H, J = 1.8 Hz), 7.99–8.05 (m, 4 H), 8.12–8.14 (d, 2 H, J = 8.4 Hz), 8.26–8.32 (m, 4 H), 8.67–8.70 (t, 4 H, J = 7.2 Hz), 8.91 (s, 4 H), 9.06–9.09 (t, 2 H, J = 4.8 Hz). MALDI TOF MS: calcd. for $C_{56}H_{38}N_4O_4S_2$ ($[M+H]^+$) 895.06; found 895.597.

Synthesis of 5,15-Bis(4′-carboxy-1,1′-biphenyl)-10,20-bis(2-thienyl) porphyrin (Por)

5,15-Bis(4′-methoxycarbonyl-1,1′-biphenyl)-10,20-bis(2-thienyl)porphyrin (**2**) (12 mg, 0.013 mmol) was dissolved in 20 mL of THF:MeOH (3:1) mixture and was hydrolyzed by 1 M NaOH at 60–70 C for 1 hr under argon atmosphere. The reaction mixture was then allowed to cool to room temperature and the organic solvent was removed under vacuum. The pH of the reaction mixture was set to pH 3–4 by adding 1 M HCl solution, and precipitate was formed. The precipitate was collected and washed several times with dilute water and dried. If necessary further purification can be carried out with column chromatography on silica gel by using DCM:hexane (2:1) as an eluent. Compound **Por** was obtained as a purple solid (11 mg, 95%). 1 H NMR (DMSO, 400 MHz): δ (ppm) = −2.79 (s, 2 H), 6.58 (s, 2 H), 6.63–6.65 (d, 2 H, J = 8.4 Hz), 6.87–6.90 (d, 4 H, J = 10.08 Hz), 7.02 (s, 4 H), 7.61–7.63 (dd, 2 H, J = 5.2 Hz), 7.86–7.88 (d, 4 H, J = 8.4 Hz), 8.04–8.07 (m, 4 H), 8.17–8.22 (m, 2 H), 8.34–8.36 (d, 2 H,

$J = 8.0$ Hz), 8.93 (s, 2 H), 9.08 (s, 2 H), 13.08 (s, 2 H). UV–vis (THF): λmax, nm (log ε, M^{-1} cm^{-1}) = 423(5.62), 518(4.32), 554(4.08), 597(3.85), 656(3.74). MALDI TOF MS: calcd. for $C_{54}H_{34}N_4O_4S_2$ ($[M+H]^+$) 867.0; found 868.618.

Synthesis of 5,15-Bis(4′-carboxy-1,1′-bipheny)-10,20-bis(2-thienyl)porphyrin zinc (ZnPor)

5,15-Bis(4′-methoxycarbonyl-1,1′-biphenyl)-10,20-bis(2-thienyl)porphyrin (**2**) (22 mg, 0.025 mmol) was dissolved in 10 mL of $CHCl_3$. To this solution 1.5 equivalent of $Zn(OAc)_2 \cdot 2\ H_2O$ prepared in 5 mL of MeOH was added. The reaction mixture was refluxed at 60–70 °C for 1 hr under Ar atmosphere. Then, the reaction mixture was allowed to cool to room temperature and the solvent was removed under vacuum. The obtained solid was dissolved in $CHCl_3$, washed twice with dilute water and dried over $MgSO_4$. $CHCl_3$ was evaporated under vacuum and the residue was purified by column chromatography on silica gel by using DCM as an eluent. The obtained porphyrin was hydrolyzed as described in Section 2.4 to give compound **ZnPor** as a purple solid (20 mg, 86%). ^{1}H NMR (DMSO, 400 MHz): δ (ppm) = 6.58 (s, 2 H), 6.63–6.65 (d, 2 H, $J = 8$ Hz), 6.87 (s, 4 H), 7.57–7.59 (m, 4 H), 7.96 (d, 2 H, $J = 2.8$ Hz), 8.11–8.19 (m, 4 H), 8.28–8.30 (d, 6 H, $J = 7.2$ Hz), 8.86–8.88 (m, 2 H), 9.01–9.03 (t, 4 H, $J = 4.6$ Hz), 13.07 (s, 2 H). UV–vis (THF): λ_{max}, nm (log ε, M^{-1} cm^{-1}) = 429(5.58), 524(3.31), 559(4.17), 601(3.73). MALDI TOF MS: calcd. for $C_{54}H_{32}N_4O_4S_2Zn$ ($[M+H]^+$) 930.37; found 931.789.

DSSC preparation

DSSC preparation started with cleaning FTO counter electrodes (TEC 8 & Hartford Glass) using Helmanex solution for 20 minutes, then rinsed and cleaned with distilled water. And then, glasses were cleaned by acetone and ethanol solvents using ultrasonic bath for 10 minutes. The TiO_2 coated FTO substrates were immersed in a 0.5 mM solution of porphyrin complexes in acetonitrile:methanol:chlorobenzene (2:2:1) at room temperature overnight and dried over $MgSO_4$ in a desicator. The active area was arranged to 0.16 cm^2 using a special mask. The cells were prepared in a sandwich geometry. The 0.6 M *N*-methyl-*N*-butylimidazolium iodide (BMII) + 0.1 M LiI + 0.05 M I2 + 0.5 M 4-tert-butylpyridine (TBP) in acetonitrile as redox electrolyte solution was introduced through pre-drilled holes in the counter electrode. The filling holes were sealed using Surlyn and a microscope cover glass.

Characterization

The NMR (400 MHz) spectra of the obtained compounds were recorded using a Bruker Ultrashield Plus Biospin GmbH spectrometer. The absorption spectra of dyes were detected on PG UV–vis spectrometer. The fluorescence spectra were measured on Varian Cary Eclipse fluorescence spectrophotometer. Mass spectra were measured using Bruker Microflex LT MALDI-TOF mass spectrometer. The electrochemical measurements were performed at room temperature on IVIUMSTAT potentiostat.

Dye-sensitized solar cells were characterized by current–voltage measurement. All current–voltage characteristics were done under 100 mW/cm^2 light intensity and AM 1.5

conditions. 450 W Xenon light source (Oriel) was used to give an irradiance of various intensities. $J-V$ data collection was made by using Keithley 2400 Source-Meter and LabView data acquisition software.

Results and discussion

The synthetic procedures of Por and ZnPor are represented in Scheme 1. First, 5-(4-bromophenyl)dipyrromethane was synthesized via the Lindsey method. Porphyrin 1 compound was synthesized by using Adler–Longo method which includes the condensation of dipyrromethane and pyrrole in propionic acid [16]. The key step is palladium-catalyzed Suzuki-Miyaura cross-coupling reaction for introducing the 4-methoxycarbonylphenyl group at the porphyrin meso position (Compound 2). The subsequent metalation by using $Zn(OAc)_2.2\ H_2O$ and base hydrolysis (NaOH) gave the zinc porphyrin (ZnPc) dye. In addition, the base hydrolysis of Compound 2 afforded the free base porphyrin (Por).

The absorption spectra of porphyrin dyes considered in this study are recorded in THF solution and shown in Fig. 1. The UV-Vis spectra of Por show characteristic Soret band at 423 nm and four *Q*-bands at 518, 554, 597, and 656 nm. On the other hand, the UV–vis spectra of ZnPor show Soret band at 429 nm and two *Q*-bands at 559 and 601 nm which are the characteristic absorption bands of metalloporphyrins. Metal center zinc (II) shifts the Soret absorption band to red region. The fluorescence spectra of porphyrins are presented in Fig. 2. The fluorescence maxima of Por and ZnPor were observed at 625 and 659 nm, respectively,

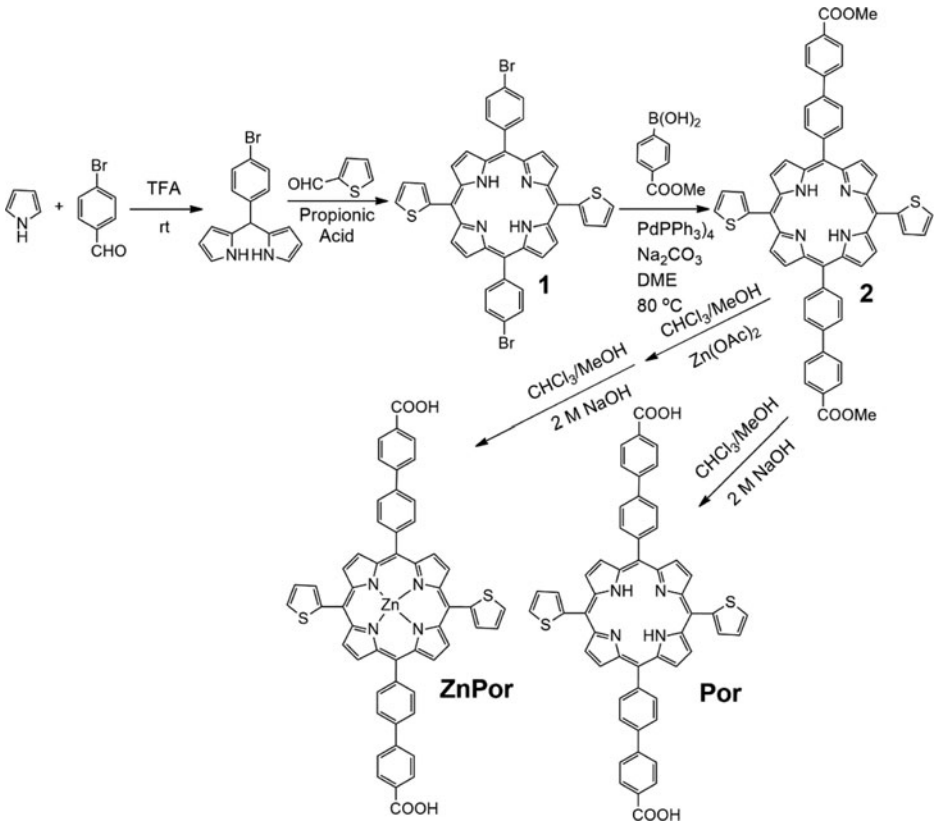

Scheme 1. Synthesis of Por and ZnPor.

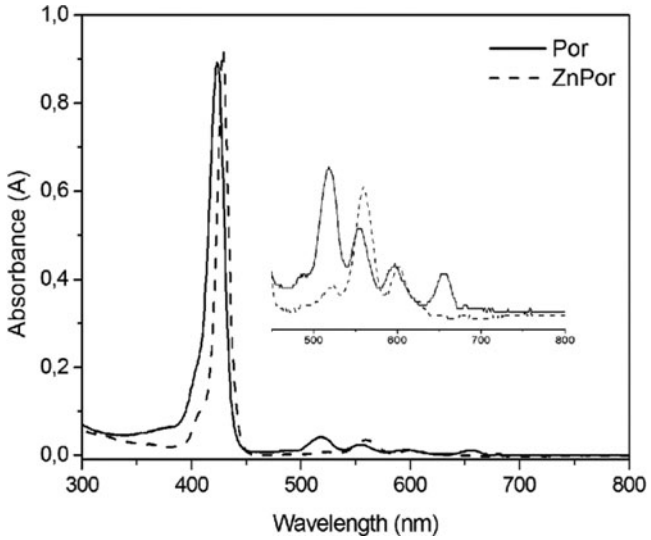

Figure 1. UV–vis absorption spectra of **Por** and **ZnPor** in THF solution.

which measured in THF solution by excitation at the Soret band. Zero–zero excitation energy (E_{0-0}) was obtained from the intersection of absorption and emission spectra (λ_{int}).

$$E_{0-0} = \frac{1240\ \text{eV}}{\lambda_{\text{int}}}$$

The calculated E_{0-0} energies of porphyrins were given in Table 1.

Cyclic voltammetry (CV) was employed to determine the electrochemical behaviors of the porphyrins. The electrochemical experiments were carried out in a typical three-electrode cell in which a glass sheet with deposited indium–tin-oxide (ITO) was used as the working electrode, a platinum wire was used as the counter electrode, an Ag/AgCl electrode was used

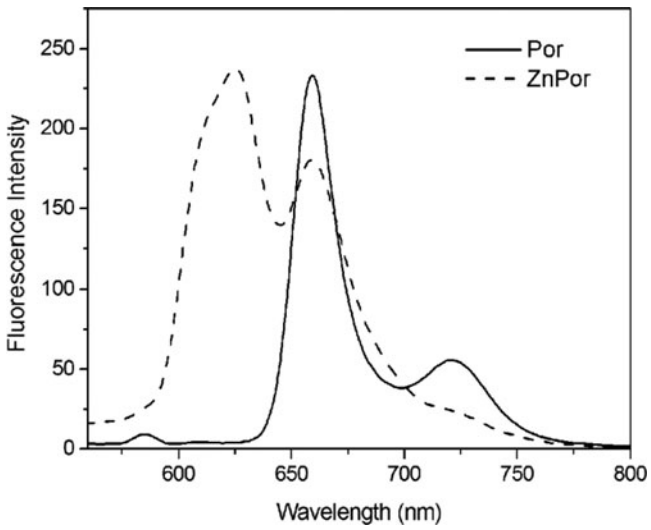

Figure 2. Fluorescence spectra of **Por** and **ZnPor** in THF solution.

Table 1. Optical and electrochemical data of **Por** and **ZnPor** in THF.

Dye	*B*-band (nm)	*Q*-band (nm)	λ_{em} (nm)	E_{ox} (V)[a]	E_{0-0} (eV)[b]	HOMO (eV)[c]	LUMO (eV)[d]
Por	423	518, 554, 597, 656	625, 659	1.05	2.02	−5.25	−3.23
ZnPor	429	559, 601	659, 721	0.91	2.07	−5.11	−3.04

[a]First oxidation onset potential vs. Ag/AgCl reference electrode.
[b]Measured from the intersection of the normalized absorption and emission spectra.
[c]HOMO $= -[(E_{ox}^{on} - E_{ferrocene}) + 4.8]$eV, where 0.6 V is the value for ferrocene vs. Ag/AgCl and 4.8 eV is the energy level of ferrocene below the vacuum.
[d]LUMO = HOMO$+E_{0-0}$.

as the reference electrode and THF containing 0.1 M tetrabuthylammonium hexaflourophosphate (TBAPF6) was used as electrolyte. Figure 3 shows the cyclic voltammograms of Por and ZnPor. The first oxidation onset potentials of Por and ZnPor were given in Table 1. The first oxidation of ZnPor shows the reversible redox process under a scan rate of 25 mV s^{-1}. However, Por shows irreversible first oxidation wave under the same condition. The highest occupied molecular orbital (HOMO) and lowest unoccupied molecular orbital (LUMO) of the dyes were also determined due to their importance in DSSC application. The HOMO energy level can be calculated from the onset oxidation potential, and values were calculated to be −5.25 and −5.11 eV for Por and ZnPor, respectively. The HOMO levels of the dyes are lower than that I^-/I^{3-} couple (−4.8 eV) [17]. This result indicated that both dyes can be efficiently regenerated by electron transfer from the electrolyte after photo oxidation. The LUMO levels were calculated from the differences between the HOMO energy levels and E_{0-0} [18]. The LUMO levels of the Por and ZnPor were estimated to be −3.23 and −3.04 eV, respectively. The LUMO levels of the dyes were higher than that of the conducting band energy of the TiO_2, suggesting that there should be enough thermodynamic driving force for electron injection from the excited state of the dyes into the conduction band of TiO_2.

In comparison with trans-2S2A [(5,15-bis(4-carboxyphenyl)-10,20-bis(2-thienyl) porphyrinato zinc(II)] reported by Ambre et al. [14], ZnPor exhibited a redshift absorption by 3 nm and lower oxidation potential. This result indicated that the use of biphenyl bridge between anchoring group and porphyrin core enhanced the conjugation length of the porphyrin macrocycle.

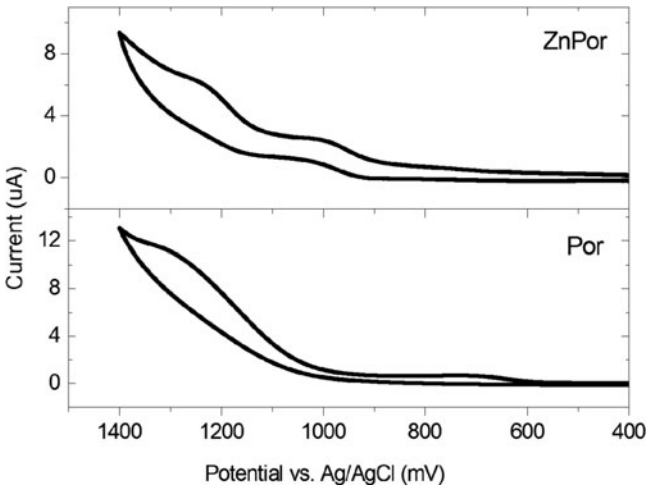

Figure 3. Cyclic voltammograms of **Por** and **ZnPor** recorded in 0.1 M TBAPF6/THF at a scan rate of 25 mV/s.

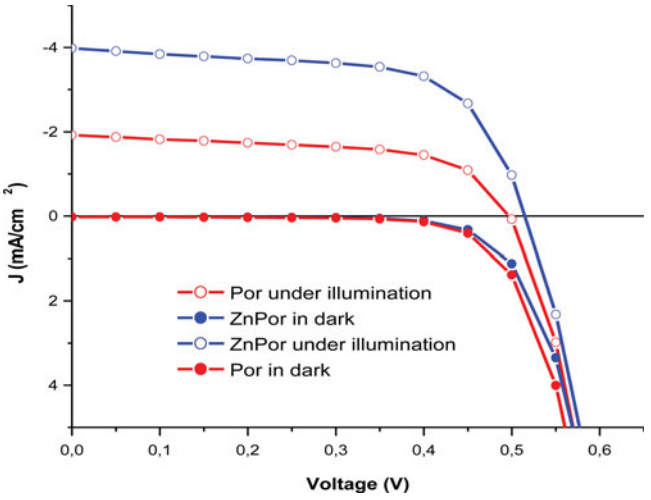

Figure 4. *J-V* curves of dye-sensitized solar cells.

The photocurrent–photovoltage (*J*–*V*) curves of porphyrin based dye sensitized solar cells were shown in Fig. 4. The detailed performance parameters including the short circuit current (J_{sc}), open-circuit photovoltage (V_{oc}), fill factor (FF), and photo to electricity conversion efficiency (η) were summarized in Table 2. According to DSSC performances, the ZnPor sensitized solar cell gave a short circuit photocurrent density, *J*sc of 3.98 mA cm^{-2}, the open circuit voltage, V_{oc} of 500 mV, and filling factor, FF of 0.67, corresponding to an overall conversion efficiency of 1.33% under the standard global AM 1.5 solar conditions. Zinc metal free complex, Por-based dye sensitized solar cell gave an overall conversion efficiency (η) of 0.58, and a short circuit photocurrent density, J_{sc} of 1.98 mA cm^{-2}, the open circuit voltage, V_{oc} of

Table 2. Photovoltaic performance of dye sensitized solar cells.

	J_{sc} (mA cm^{-2})	V_{oc} (mV)	FF	η (%)
Por	1.92	500	0.60	0.58
ZnPor	3.98	500	0.67	1.33

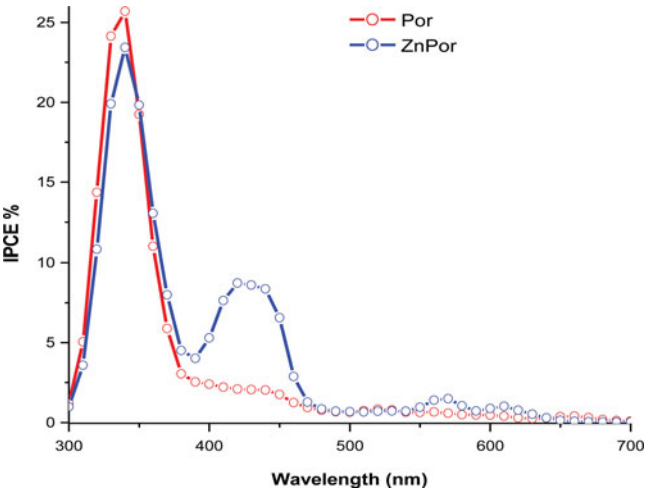

Figure 5. Incident photon to charge carrier efficiency of dye-sensitized solar cells.

500 mV and filling factor, FF of 0.60. In this study, we investigated the central metal effect in dye sensitized solar cells. Our results show that central zinc metal increased the efficiency in dye sensitized solar cells.

Overall conversion efficiencies were obtained as 1.33% and 0.58%, respectively. These performances are actually in accord with those obtained in IPCE spectrum. IPCE spectrum of porphyrin based dye sensitized solar cells was presented in Fig. 5. ZnPor and Por showed IPCE efficiencies of 8.79% and 2.39% at 429 nm, respectively.

Conclusion

In summary, new porphyrin dyes Por and ZnPor were synthesized and applied in DSSC. 0.58% and 1.33% of light to electricity conversion efficiencies were achieved for Por and ZnPor, respectively. It was found that Zn(II) shifted the Soret absorption band to the red region and decreased the band gap energy of porphyrin. Based on these results, ZnPor exhibited better conversion efficiency in DSSC. In addition to thienyl group, biphenyl group also enhanced the conjugation length. Our studies will go on through a rational molecular design of new porphyrin dyes for higher efficiencies in dye sensitized solar cells.

References

[1] Grätzel, M. (2003). *J. Photochem. Photobiol. C Photochem. Rev.*, *4*, 145.
[2] Erten-Ela, S., & Cakir, A. C. (2015). *Energy Sources, 37*, 807.
[3] Erten-Ela, S. (2014). *International Journal of Photoenergy*, Article ID 941213, 6 pages, http://dx.doi.org/10.1155/2014/941213.
[4] Erten-Ela, S., & Sarica, H. (2012). *Journal of Optoelectronics and Advanced Materials, 14*, 753.
[5] Erten-Ela, S. (2013). *International Journal of Photoenergy*, Article ID 436831, 6 pages, http://dx.doi.org/10.1155/2013/436831
[6] Campbell, W. M., Jolley, K. W., Wagner, P., Wagner, K., Walsh, P. J., et al. (2007). *J. Phys. Chem. C.*, *36*(3), 11760.
[7] Mathew, S., Yella, A., Gao, P., Humphry-Baker, R., Curchod, B. F. E., et al. (2014). *Nat. Chem.*, *6*(3), 242.
[8] Yella, A., Lee, H.-W., Tsao, H. N., Yi, C., Chandiran, A. K., et al. (2011). *Science*, *334*, 629.
[9] Imahori, H., Hayashi, S., Hayashi, H., Oguro, A., Eu, S., et al. (2009). *J. Phys. Chem. C.*, *113*, 18406.
[10] Nazeeruddin, M. K., Humphry-Baker, R., Officer, D. L., Campbell, W. M., Burrell, A. K., et al. (2004). *Langmuir*, *20*(15), 6514.
[11] Rochford, J., Chu, D., Hagfeldt, A., & Galoppini, E. (2007). *J. Am. Chem. Soc.*, *129*(15), 4655.
[12] Boyle, N. M., Rochford, J., & Pryce, M. T. (2010). *Coord. Chem. Rev.*, *254*(1–2), 77.
[13] Cogal, S., Erten-Ela, S., Ocakoglu, K., & Uygun, A. (2015). *Dye. Pigment.*, *113*, 474.
[14] Ambre, C.-H., Chen, K.-B., Yao, C.-F., Luo, L., Diau, E. W-G., et al. (2012). *J. Phys. Chem. C.*, *116*, 11907.
[15] Littler, B. J., Miller, M. A., Hung, C., Wagner, R. W., Shea, D. F. O., et al. (1999). *J. Org. Chem.*, *64*, 1391.
[16] Bhyrappa, P., & Bhavana, P. (2001). *Chem. Phys. Lett.*, *349*, 399.
[17] Balanay, M. P., & Kim, D. H. (2008). *Phys. Chem. Chem. Phys.*, *10*(33), 5121.
[18] a) Ocakoglu, K., Erten-Ela, S., Joya, K. S, & Harputlu, E. (2016). *Inorganica Chimica Acta, 439*, 30. b) Erten-Ela, S., Vakuliuk, O., Tarnowska, A., Ocakoglu, K., & Gryko, D. T. (2015). *Spectrochimica Acta Part A: Molecular and Biomolecular Spectroscopy, 135*, 676.